

# An Integrated Bidirectional Bridge with Dual RMS Detectors for RF Power and Return-Loss Measurement

By **Eamon Nash** and **Eberhard Brunner**

Share on   

Directional couplers are used in a wide variety of applications to sense RF power, and they may appear at multiple points in a signal chain. In this article, we will explore the **ADL5920**, a new device from Analog Devices that combines a broadband directional bridge-based coupler with two rms responding detectors in a 5 mm × 5 mm surface-mount package. This device offers significant advantages over conventional discrete directional couplers that struggle with the trade-off between size and bandwidth, particularly at frequencies below 1 GHz.

In-line RF power and return loss measurements are typically implemented using directional couplers and RF power detectors.

In Figure 1, a bidirectional coupler is used in a radio or test and measurement application to monitor transmitted and reflected RF power. It's also sometimes desirable to have RF power monitoring embedded in a circuit, with a good example being where two or more sources are being switched into the transmit path (either using an RF switch or with external cables).

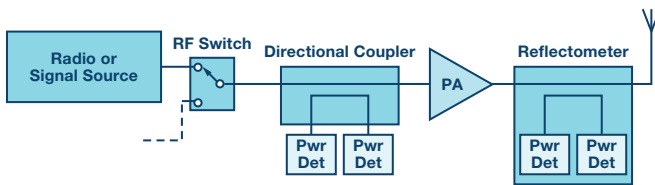


Figure 1. Measuring forward and reflected power in an RF signal chain.

Directional couplers have the valuable characteristic of directivity—that is, the ability to distinguish between incident and reflected RF power. As the incident RF signal travels through the forward path coupler on its way to the load (Figure 2), a small proportion of the RF power (usually a signal that is 10 dB to 20 dB lower than the incident signal) is coupled away and drives an RF detector. Where both forward and reflected power are being measured, a second coupler with reverse orientation compared to the forward path coupler is used. The output voltage signals from the two detectors will be proportional to the forward and reverse RF power levels.

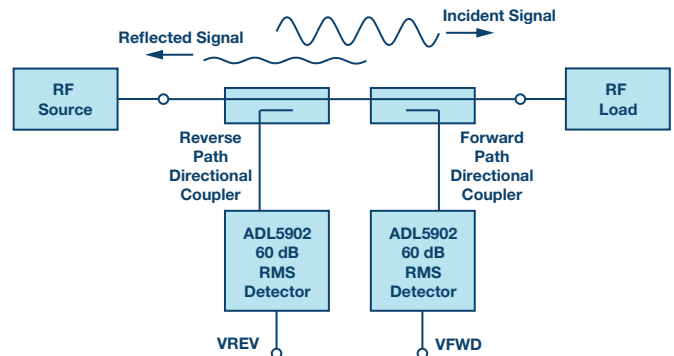


Figure 2. A typical RF power measurement system using directional couplers and RF detectors.

Surface-mount directional couplers suffer from a fundamental trade-off between bandwidth and size. While bidirectional directional couplers with one octave of frequency coverage (that is,  $F_{MAX}$  is equal to twice  $F_{MIN}$ ) are commonly available in packages as small as 6 mm<sup>2</sup>, a multioctave surface-mount directional coupler will be much larger (Figure 3). Broadband connectorized directional couplers have multioctave frequency coverage but are significantly larger than surface-mount devices.

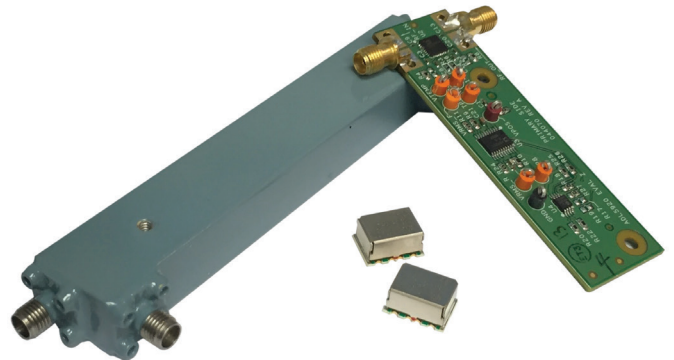


Figure 3. Connectorized directional coupler, surface-mount directional coupler, and ADL5920 integrated IC with directional bridge and dual rms detectors.

Figure 3 also shows the evaluation board for the ADL5920, a new RF power detection subsystem with up to 60 dB of detection range, packaged in a 5 mm × 5 mm MLF package (the ADL5920 IC is located between the RF connectors). The block diagram for the ADL5920 is shown in Figure 4.

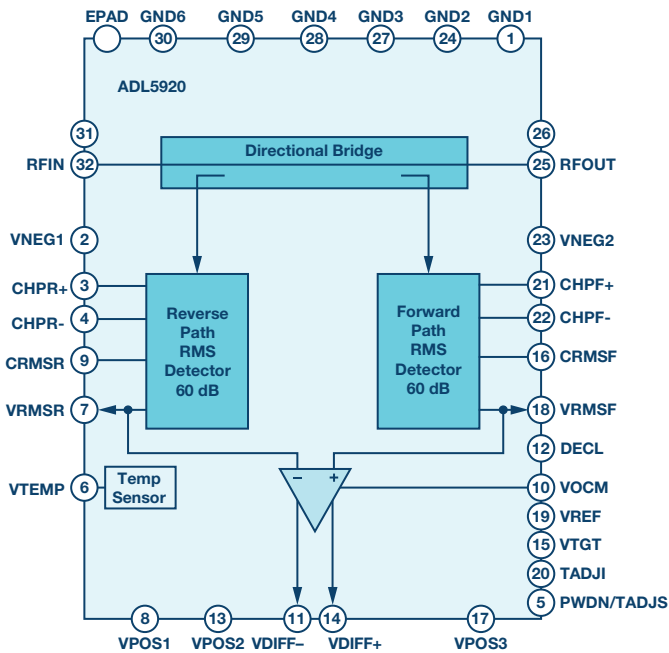


Figure 4. ADL5920 block diagram.

Instead of sensing the forward and reflected signals using directional couplers, the ADL5920 uses a patented directional bridge technology to achieve broadband and compact on-chip signal coupling. To understand how a directional bridge works, we need to first take a step back and look at the Wheatstone bridge.

### Wheatstone Bridge

The notion of a directional bridge is based on the Wheatstone bridge (Figure 5) that creates zero differential voltage when balanced. In a Wheatstone bridge, one resistor in one of the two legs is variable ( $R_2$ ), while two others ( $R_1$  and  $R_3$ ) are fixed. There are four resistors in total— $R_1$ ,  $R_2$ ,  $R_3$ , and  $R_x$ —where  $R_x$  is an unknown resistance. If  $R_1 = R_3$ , then when  $R_2$  is equal to  $R_x$ ,  $V_{OUT} = 0$  V. The bridge is considered balanced when the variable resistor is of the correct value such that the voltage divide ratios on the left and right side of the bridge are equal and thereby create a zero volt differential signal across the differential sense nodes that produce  $V_{OUT}$ .

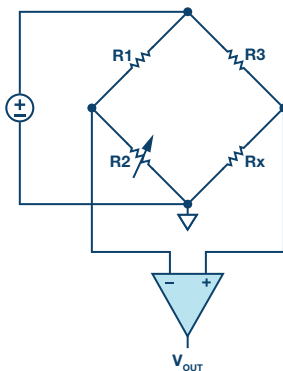


Figure 5. Wheatstone bridge.

### A Unidirectional Bridge

Figure 6 is the schematic of a unidirectional bridge and it best explains the basic operation of such a device. First, it is important to observe that a directional bridge needs to be designed for a particular  $Z_0$  and that insertion loss is minimized. If  $R_s = R_l = R = 50 \Omega$ , then the sense resistor of the bridge is  $5 \Omega$ , which is a good compromise between insertion loss ( $<1$  dB) and signal sensing. Calculating  $R_{OUT}$  as seen looking back from the load results in an exact  $50 \Omega$  port impedance, while calculating  $R_{IN}$  will result in  $50.8 \Omega$  port impedance ( $|\Gamma| = 0.008$ ;  $RL = -42$  dB;  $VSWR = 1.016$ ). If a signal is applied as shown at RFIP then, since  $R_{IN} \sim 50 \Omega$ , the voltage at RFIP is about half of the source voltage. If we assume for a moment that the voltage at RFIP equals  $1$  V, then the voltage at RFOP will be about  $0.902$  V.

This voltage is further attenuated by  $10/11 = 0.909$  such that the negative input of the differencing amplifier is  $0.82$  V with a resultant differential voltage of  $(1 - 0.82) = 0.18$  V. The effective forward coupling factor ( $Cpl$ ) of this bridge is

$$Cpl = 20 \log_{10} \left( \frac{0.18 \text{ V}}{1 \text{ V}} \right) = 15 \text{ dB} \quad (1)$$

Balanced in the context of the bridge means that when a signal is applied in the reverse direction (RFOP to RFIP), then the VFWD detector (or  $Cpl$  port) will ideally see zero differential voltage, while it sees a maximum signal when the signal is applied in the forward direction (RFIP to RFOP). To get maximum directivity in such a structure, precision resistors are of utmost importance and that is why integrating them is beneficial.

In a unidirectional bridge, to determine isolation, which is needed to calculate return loss, one needs to flip the device and then apply the input signal to RFOP. In that case, the bridge is balanced and the plus and minus inputs to the differential amplifier are equal, since the same divide ratios of  $0.909 = (10R/(10R + R)) = (R/(R+0.1R))$  result in a differential voltage of  $(V_+ \text{ minus } V_-) = 0$  V.

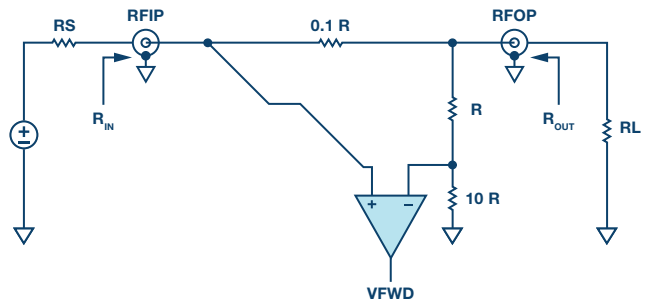


Figure 6. Simplified unidirectional bridge diagram.

### A Bidirectional Bridge

Figure 7 is a simplified diagram of a bidirectional bridge, similar to the one used in the ADL5920. The unit resistance  $R$  is equal to  $50 \Omega$  for a  $50 \Omega$  environment. So the value of the bridge's sense resistor is  $5 \Omega$ , while the two shunt-networks are each about  $1.1$  k $\Omega$ .

This is a symmetric network, so the input and output resistances,  $R_{IN}$  and  $R_{OUT}$ , are the same and close to  $50 \Omega$  when  $R_s$  and  $R_l$  are also equal to  $50 \Omega$ .

When the source and load impedance are both  $50 \Omega$ , an ohmic analysis of the internal network tells us that VFWD will be quite large compared to VREV. In a real-world application, this corresponds to maximum power transmission from source to load. This results in reflected power that is small, which in turn results in a very small VREV.

Next, let's consider what happens if  $R_L$  is either infinite (open circuit) or zero (shorted load). In both cases, if we repeat the ohmic analysis, we find that VFWD and VREV are approximately equal. This mirrors a real-world system where an open or shorted load results in forward and reflected power being equal. A more detailed analysis of these scenarios follows below.

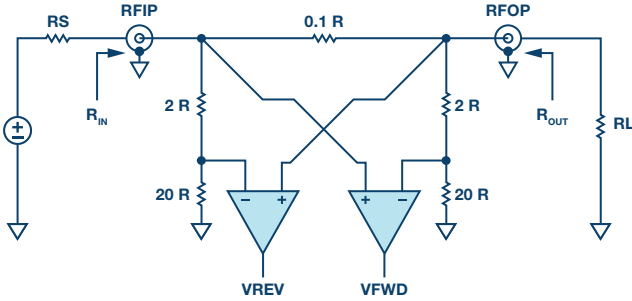


Figure 7. Simplified bidirectional bridge diagram.

### VSWR and Reflection Coefficient

A full analysis of errors in network analysis is too complicated and beyond the scope of this article, yet we want to summarize some of the basic concepts here. An excellent resource is the application note by Marki Microwave, *Directivity and VSWR Measurements*.<sup>1</sup>

Traveling waves are important concepts to describe the voltages and currents along transmission lines since they are functions of position and time. The general solution of voltages and currents along transmission lines consist of a forward traveling wave and a reverse traveling wave, which are functions of distance  $x$ .<sup>2</sup>

$$V(x) = V^+(x) + V^-(x) \quad (2)$$

$$I(x) = \frac{V^+(x)}{Z_0} - \frac{V^-(x)}{Z_0} \quad (3)$$

In Equation 2 and Equation 3,  $V^+(x)$  represents the voltage wave traveling toward the load, while  $V^-(x)$  represents the voltage wave reflected from the load due to mismatch, and  $Z_0$  is the characteristic impedance of the transmission line. In a lossless transmission line,  $Z_0$  is defined by the classic equation:

$$Z_0 = \sqrt{\frac{L}{C}} \quad (4)$$

The most common  $Z_0$  is 50  $\Omega$  for transmission lines. If such a line is terminated with its characteristic impedance, then it appears to a 50  $\Omega$  source as an infinite line since any voltage wave traveling down the line will not result in any reflections that can be sensed at the source or anywhere else along the line. However, if the load is different from 50  $\Omega$ , then a standing wave will be generated along the line that can be detected and is defined by the voltage standing wave ratio (VSWR).

More generally, the reflection coefficient is defined as:

$$\Gamma(x) = \Gamma_0 e^{2\gamma x} \quad (5)$$

where  $\Gamma_0$  is the load reflection coefficient and  $\gamma$  the propagation constant of the transmission line.

$$\Gamma_0 = \frac{Z_L - Z_0}{Z_L + Z_0} \quad (6)$$

$$Z_0 = \sqrt{\frac{R + j\omega L}{G + j\omega C}} \quad (7)$$

$$\gamma = \sqrt{(R + j\omega L)(G + j\omega C)} \quad (8)$$

$R$ ,  $L$ ,  $G$ , and  $C$  are the resistance, inductance, conductance, and capacitance per unit length of the transmission line.

The return loss (RL) is the negative of the reflection coefficient ( $\Gamma$ ) in dB. This is important to point out as reflection coefficient and return loss are frequently confused and used interchangeably.

$$RL = -20 \log_{10} |\Gamma_0| = 10 \log_{10} \frac{1}{|\Gamma_0|^2} \quad (9)$$

Another very important definition of return loss in addition to the load mismatch above is in terms of incident and reflected power at an impedance discontinuity. This is given by

$$RL = 10 \log_{10} \left( \frac{P_{incident}}{P_{reflected}} \right) \quad (10)$$

and extensively used in antenna design. VSWR, RL, and  $\Gamma_0$  are related as follows:

$$|\Gamma_0| = \frac{VSWR - 1}{VSWR + 1} \quad (11)$$

$$VSWR = \frac{|V(x)|_{max}}{|V(x)|_{min}} + \frac{1 + |\Gamma_0|}{1 - |\Gamma_0|} = \frac{1 + 10^{-\frac{RL}{20}}}{1 - 10^{-\frac{RL}{20}}} \quad (12)$$

$$RL = -20 \log_{10} \left( \frac{VSWR - 1}{VSWR + 1} \right) \quad (13)$$

Equation 14 and Equation 15 represent the maximum and minimum of the standing wave voltages. VSWR is defined as the ratio of the maximum to the minimum voltage along the wave. The peak and minimum voltages along the line are

$$|V(x)|_{max} = |A|(1 + |\Gamma_0|) \quad (14)$$

$$|V(x)|_{min} = |A|(1 - |\Gamma_0|) \quad (15)$$

For example, in a 50  $\Omega$  transmission line, if the forward traveling voltage signal has a peak amplitude of  $A = 1$  and the line is matched with a perfect load, then  $|\Gamma_0| = 0$ , there is no standing wave (VSWR = 1.00), and the peak voltage along the line is  $A = 1$ . However, if  $R_{LOAD}$  is 100  $\Omega$  or 25  $\Omega$ , then  $|\Gamma_0| = 0.333$ , RL = 9.542 dB, and VSWR = 2.00, with  $|V(x)|_{max} = 1.333$  and  $|V(x)|_{min} = 0.666$ .

Figure 8 is a replica of Figure 7 but with signals shown in the default forward configuration and with traveling power waves indicated where the reference plane is at the load. At low frequencies where the wavelength is long relative to the physical structure, voltages, and currents are in phase and the circuit can be analyzed according to Ohm's law.

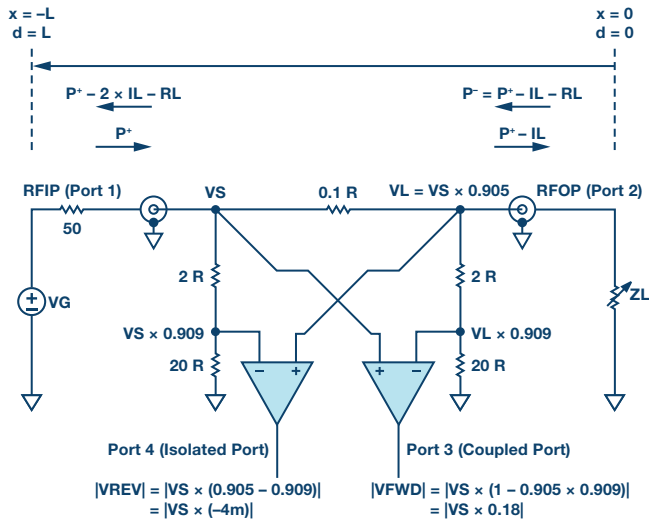


Figure 8. Simplified bidirectional bridge with signals.

The ports are defined as shown with the input port (Port 1) at RFIP, output port (Port 2) at RFOP, coupled port (Port 3) at  $V_{FWD}$ , and isolated port (Port 4) at  $V_{REV}$ . Since the structure is symmetric, the ports are reversed when a signal is reflected at  $Z_L$  or applied to RFOP.

In the case of a matched load, and the generator voltage connected to Port 1 (RFIP), and with  $Z_s = Z_L = Z_0 = R = 50 \Omega$ ,

$$V_L = V_{S+} \left[ \frac{Z_{OUT}}{Z_{OUT} + 0.1R} \right] = V_{S+} \times 0.905 = V_{S+} \times |S_{21}| \quad (16)$$

$$Z_{OUT} = Z_L \parallel (2R + 20R) = R \parallel 22R = \left( \frac{22}{23} \right) R \quad (17)$$

and  $V_L/V_{S+}$  is the insertion loss,  $L_1$ , or  $IL$  in dB.

$$IL = -20 \log_{10} |S_{21}| = -20 \log_{10} L_1 = 0.87 \text{ dB} \quad (18)$$

The attenuation factor for the two shunt legs on either side of the main line resistor of  $0.1 \times R$  is

$$\alpha = \frac{20R}{(20R + 2R)} = \frac{20}{22} = 0.909 \quad (19)$$

The equations in Figure 8 for  $|V_{REV}|$  and  $|V_{FWD}|$  show the values for those voltages with a signal applied in the forward direction. These equations indicate a fundamental directivity limit for the simplified schematic due to nonideal rejection at the isolated port of 33 dB.

$$D = 20 \log_{10} \left( \frac{|V_{CPL}|}{|V_{ISO}|} \right) = 20 \log_{10} \left( \frac{|0.18|}{|-0.004|} \right) = 33 \text{ dB} \quad (20)$$

From Figure 8, one can see that the directivity of the bidirectional bridge in the linear domain is determined by

$$D_L = \left( \frac{1 - L_1 \times \alpha}{L_1 - \alpha} \right) \quad (21)$$

which shows that to increase directivity,  $\alpha$  needs to equal the insertion loss,  $L_1$ .

In silicon, the peak directivity is typically better than the simplified diagram would indicate (Figure 9).

If  $Z_L$  is not equal to  $Z_0$ , as is normally the case, the coupled and isolated port voltages, which are complex, would be

$$V_{CPL} = V_{S+}[1 - L_1 \times \alpha] + V_{L-}[L_1 - \alpha] \quad (22)$$

$$V_{ISO} = V_{L-}[1 - L_1 \times \alpha] + V_{S+}[L_1 - \alpha] \quad (23)$$

where  $V_{S+}$  is the forward voltage at Port 1 (node  $V_S$ ) and  $V_{L-}$  is the reflected voltage from the load at Port 2 (node  $V_L$ ).  $\Theta$  is the unknown phase of the reflected signal,

$$V_{L-} = V_{S+} \times L_1 \times |\Gamma_0| e^{j\Theta} \quad (24)$$

Substituting (24) for  $V_{L-}$  in (22) and (23) and using (21) to simplify the result, plus the fact that

$$V_{FWD} = V_{S+}[1 - L_1 \times \alpha] \quad (25)$$

results in complex output voltages

$$V_{CPL} = V_{FWD} \left\{ 1 + \frac{L_1 \times |\Gamma_0| e^{j\Theta}}{D_L} \right\} \quad (26)$$

$$V_{ISO} = V_{FWD} \left\{ L_1 \times |\Gamma_0| e^{j\Theta} + \frac{1}{D_L} \right\} \quad (27)$$

From (26) and (27) we can observe that for  $D_L \gg 1$ ,

$$\left| \frac{V_{ISO}}{V_{CPL}} \right|_{max, min} = \sqrt{\frac{\left( \frac{1}{D_L} \right)^2 \pm 2 \left( \frac{L_1 \times |\Gamma_0|}{D_L} \right) + (L_1 \times |\Gamma_0|)^2}{1 + 2 \left( \frac{L_1 \times |\Gamma_0|}{D_L} \right) + \left( \frac{L_1 \times |\Gamma_0|}{D_L} \right)^2}} \rightarrow L_1 \times |\Gamma_0| \quad (28)$$

In the ADL5920, the voltages  $V_{REV}$  and  $V_{FWD}$  are mapped via two 60 dB range linear-in-dB rms detectors into voltages  $V_{RMSR}$  and  $V_{RMSF}$  that are  $(V_{ISO}/V_{SLP})$  and  $(V_{CPL}/V_{SLP})$  in dB, respectively. So the differential output of the device  $V_{DIFF}$  in dB represents

$$\frac{V_{DIFF}}{V_{SLP}} = \frac{V_{RMSR} - V_{RMSF}}{V_{SLP}} = \frac{V_{L_1} + V_{|\Gamma_0|}}{V_{SLP}} \quad (29)$$

where  $V_{SLP}$ , the detector slope, is about 60 mV/dB.

Using the voltage-to-dB mapping of (29) in (28)

$$20 \log_{10} \left( \frac{V_{RMSR}}{V_{SLP}} \right) - 20 \log_{10} \left( \frac{V_{RMSF}}{V_{SLP}} \right) = 20 \log_{10}(L_1) + 20 \log_{10}|\Gamma_0| \quad (30)$$

And using Equation 9 in Equation 30 results in

$$P_{REV} - P_{FWD} = -IL - RL \quad (31)$$

$$RL = P_{FWD} - P_{REV} - IL \quad (32)$$

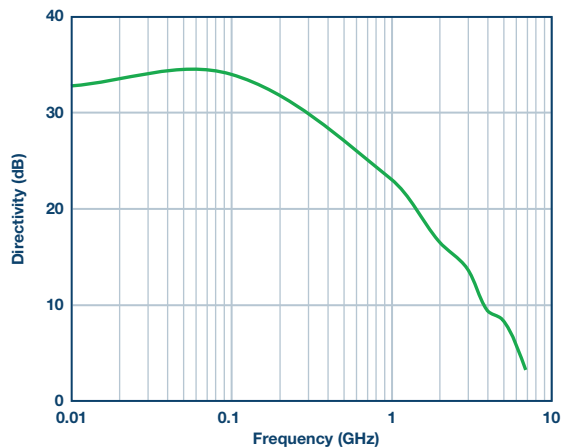


Figure 9. ADL5920 directivity vs. frequency. The input level is 20 dBm.

Figure 10 shows the response of the forward power sensing rms detector when the ADL5920 is driven in the forward direction. Each trace corresponds to the output voltage vs. frequency for a particular power level applied. While the plot stops at 10 MHz, operation at frequencies down to 9 kHz has been verified. In Figure 11, the same data is presented as output voltage vs. input power with each trace representing a different frequency.

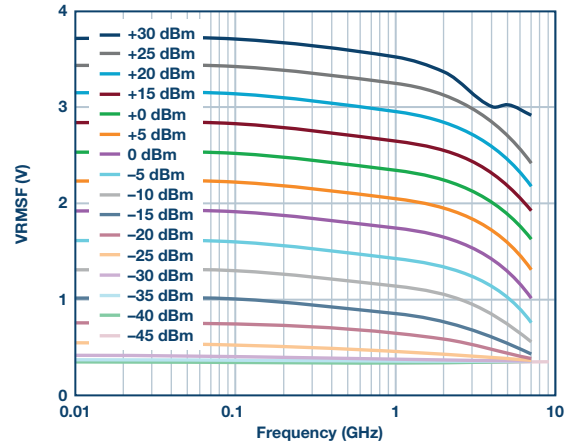


Figure 10. Typical output voltage vs. frequency from forward path detector at multiple input power levels.

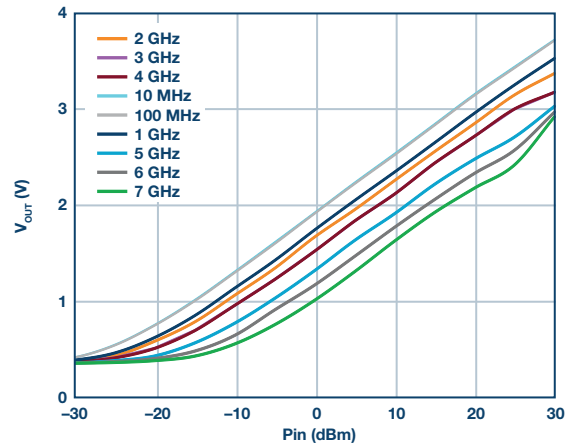


Figure 11. Typical output voltage vs. input power from forward path detector at multiple frequencies.

When the ADL5920's  $RF_{OUT}$  pin is terminated with a  $50 \Omega$  resistor, there should be no reflected signal. Therefore, the reverse path detector should not register any detected reverse power. However, because the directivity of the circuit is nonideal and rolls off vs. frequency, some signal will be detected in the reverse path. Figure 12 shows the voltage measured on the forward and reverse path detectors at 500 MHz when  $RF_{IN}$  is swept and  $RF_{OUT}$  is terminated with  $50 \Omega$ . The vertical separation between these traces relates directly to the directivity of the bridge.

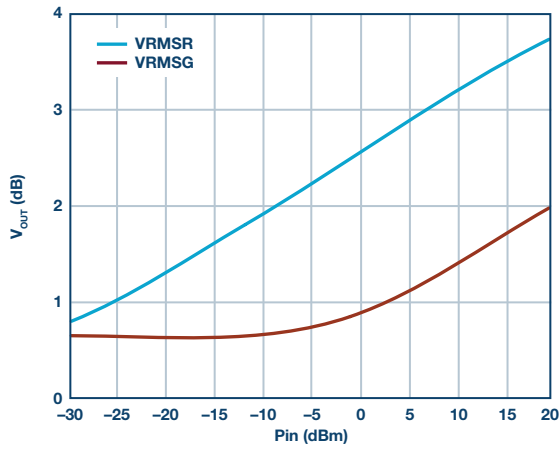


Figure 12. VRMSF and VRMSR output voltage vs. input power at 500 MHz when the bridge is driven from  $RF_{IN}$  and  $RF_{OUT}$  is terminated with 50  $\Omega$ .

Figure 13 shows the effect of varying the load on the measurement of forward power. Defined power levels are applied to the  $RF_{IN}$  input and the return loss of the load on  $RF_{OUT}$  is varied from 0 dB to 20 dB. As expected, when the return loss is in the 10 dB to 20 dB range, the power measurement accuracy is quite good. But as the return loss is reduced below 10 dB, the power measurement error starts to increase. It is notable that for a return loss of 0 dB, the error is still only in the 1 dB range.

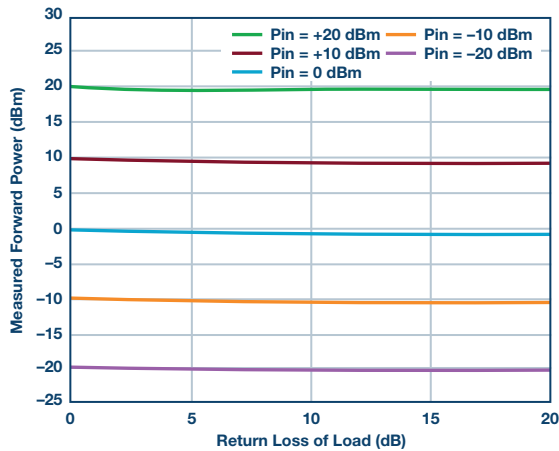


Figure 13. Measured forward power vs. applied power and return loss of load, measured at 1 GHz.

In Figure 14, the ADL5920 is being used to measure the return loss of the load, also at 1 GHz. A known return loss is applied to the  $RF_{OUT}$  port. VRMSF and VRMSR are measured and the return loss is back calculated.

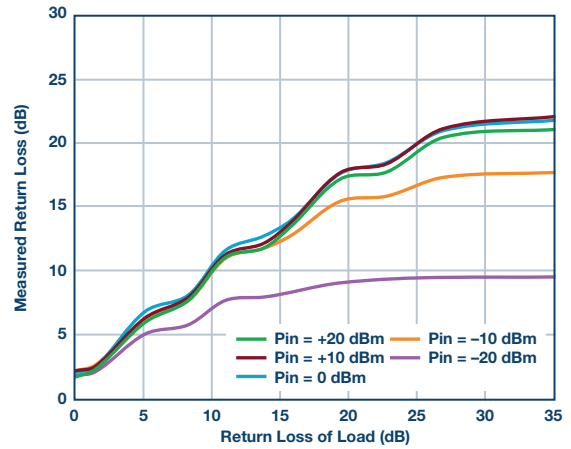


Figure 14. Measured return loss vs. applied return loss and RF power, measured at 1 GHz.

There are a number of points to note about this plot. Firstly, it can be seen that the ADL5920's ability to measure return loss degrades as the return loss improves. This is due to the directivity of the device. Secondly, note how the measurement accuracy degrades as the drive power drops. This is due to the limited detection range and sensitivity of the ADL5920 on-board rms detectors. The third observation relates to the apparent ripple in the traces. This is caused by the fact that each measurement is being taken at a single return loss phase. If the measurement was repeated at all return loss phases, a family of curves would result whose vertical width would be roughly equal to the vertical width of the ripple.

## Applications

With the ability to measure inline RF power and return loss, the ADL5920 is useful for multiple applications. Its small size means that it can be dropped into many circuits without having a significant space impact. Typical applications include in-circuit RF power monitoring at RF power levels up to 30 dBm, where insertion loss is not critical. The return loss measurement capability is typically used in applications where an RF load is being monitored. This could be a simple circuit to check that an antenna has not been damaged or broken off (that is, catastrophic failure). However, ADL5920 can also be used to measure scalar return loss in materials analysis applications. This is most applicable at frequencies below approximately 2.5 GHz where the directivity (and thereby the measurement accuracy) is greater than 15 dB.

The ADL5920 is available to evaluate in two form factors, as shown in Figure 15. The left side shows the traditional evaluation board where the detector output voltages are available on clip leads and SMA connectors. This evaluation board also includes a calibration path which can be used to calibrate out the insertion loss of the FR4 board.

The right side shows a more integrated evaluation board that includes a 4-channel, 12-bit ADC (AD7091R-4). This evaluation board plugs into the Analog Devices SDP-S USB interface board and includes PC software that calculates RF power and return loss and includes a basic power calibration routine.

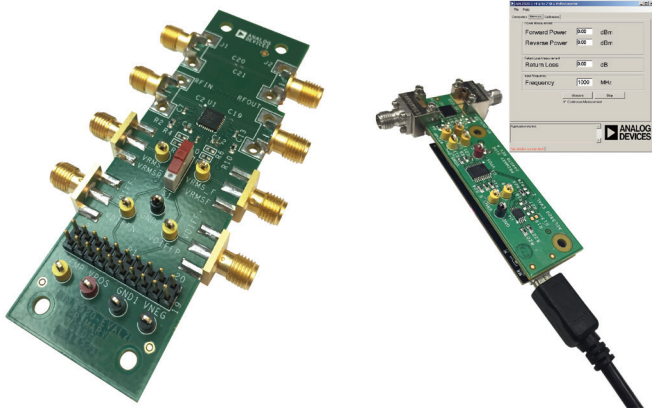


Figure 15. ADL5920 evaluation board options.

## References

- <sup>1</sup> Doug Jorgesen and Christopher Marki. *Directivity and VSWR Measurements: Understanding Return Loss Measurements*. Marki Microwave, 2012.
- <sup>2</sup> Guillermo Gonzalez. *Microwave Transistor Amplifiers Analysis and Design*. Prentice-Hall, 1984.
- <sup>3</sup> Eamon Nash. “*Understanding, Operating, and Interfacing to Integrated Diode-Based RF Detectors*.” Analog Devices, Inc., November 2015.

## Acknowledgements

We would like to thank Steve Boyle for thoughtful discussions and constructive inputs, and Rob Hicks for creation of the evaluation board. Furthermore, we are forever indebted to Peter Kearney for all his measurements.

Eamon Nash [eamon.nash@analog.com] is an applications engineering director at Analog Devices. He has worked at Analog Devices for 28 years in various field and factory roles covering mixed signal, precision, and RF products. He currently works in ADI's RF Products Group, specializing in RF power measurement, phased array radar, and millimeter wave imaging. He holds a Bachelor of Engineering degree in electronics from University of Limerick, Ireland.



Eamon Nash

Eberhard Brunner [eberhard.brunner@analog.com] is a senior design engineer at Analog Devices, with a B.S.E.E. from UC Berkeley (1988) and an M.S.E.E. from Oregon Graduate Institute (1995). He is also an alumnus of Santa Clara University. After graduation from UC Berkeley, he worked for Harris Farinon, a microwave radio company, as a modem design engineer. In 1991 he moved to Oregon and joined Analog Devices' northwest labs, reporting to ADI Fellow Barrie Gilbert. Since this time, he has worked as a technician and applications engineer, in product engineering support, marketing, and mostly design. His areas of expertise are in nonlinear analog design, RF power detection, medical imaging, and microwave design. He currently works in the Power over Ethernet (PoE) design group in Santa Barbara, CA. He has 10 issued patents.



Eberhard Brunner